Electronic Supplementary Information:

Fine-grained and fully ordered intermetallic PtFe catalyst with largely enhanced catalytic activity and durability

Xin Xin Du,† Yang He,† Xiao Xia Wang, Jian Nong Wang*

Nano Carbon Research Center, School of Mechanical and Power Engineering, East China University of Science and Technology, 130 Meilong Road, Shanghai 200237, P. R. China.

* Corresponding author. Tel: +86-21-64252360. E-mail: jnwang@ecust.edu.cn

† These authors contributed equally to this work.

Calculations of I_k, S_a, M_a, and n

To compare the catalytic activities of different catalysts, some activity values were calculated. The kinetic current (I_k) was calculated using the Koutecky-Levich equation:

$$\frac{1}{I} = \frac{1}{I_k} + \frac{1}{I_d}$$

(1)

where I is the experimentally measured current, and I_d the diffusion limiting current density.

The specific activity (S_a) was calculated by the following equation:

$$S_a = \frac{I_k}{ECSA \times m}$$

(2)

where $ECSA$ is the electrochemically active surface area and m is the Pt loading on the working electrode. $ECSA$ could be estimated from the CV curve by the following equation:

$$ECSA = \frac{Q}{m \cdot \beta}$$

(3)

where Q is the charge of hydrogen desorption, and β the charge required to oxidize a monolayer of H_2 on bright Pt (assumed to be 210 µC cm^{-2}). The Q value can be calculated from the cyclic voltamogram without inclusion of the contribution of the charge from the electric double layer.
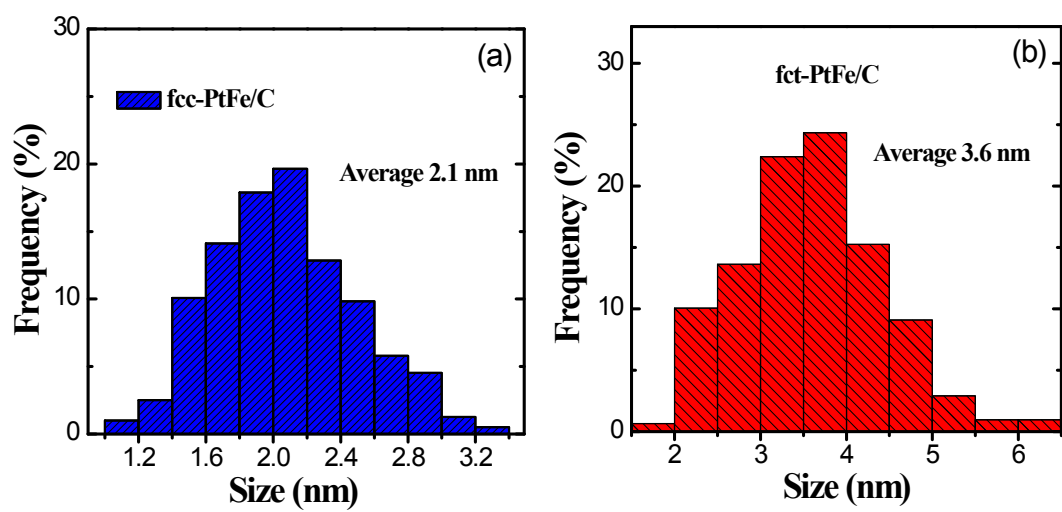
The mass activity (M_a) was calculated by the following equation:
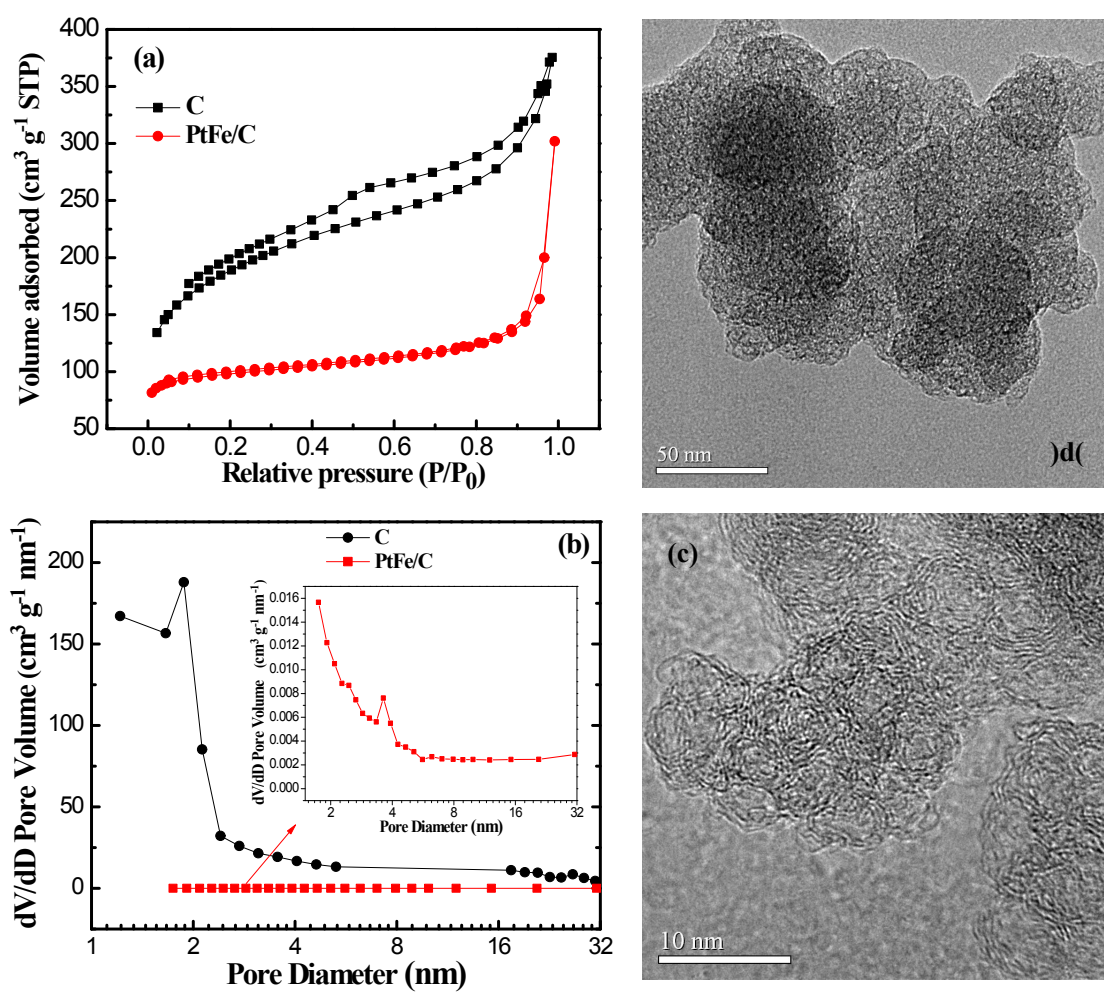
$$M_a = \frac{I_k}{m}$$

(4)

The enhancement factor (n) was defined as the ratio of the mass activity of the prepared catalyst (M_a) and that of the commerical Pt/C catalyst (M_a^*):
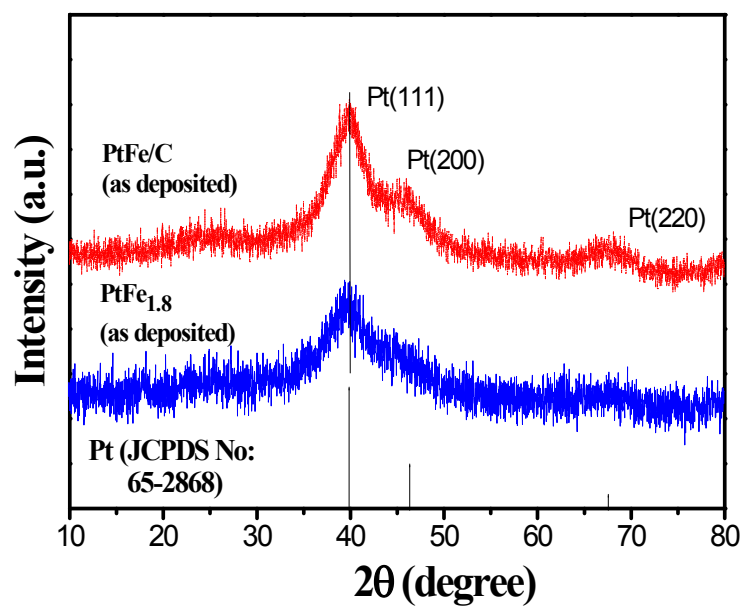
$$n = \frac{M_a}{M_a^*}$$

(5)

These two catalysts were tested under identical conditions in the same laboratory.
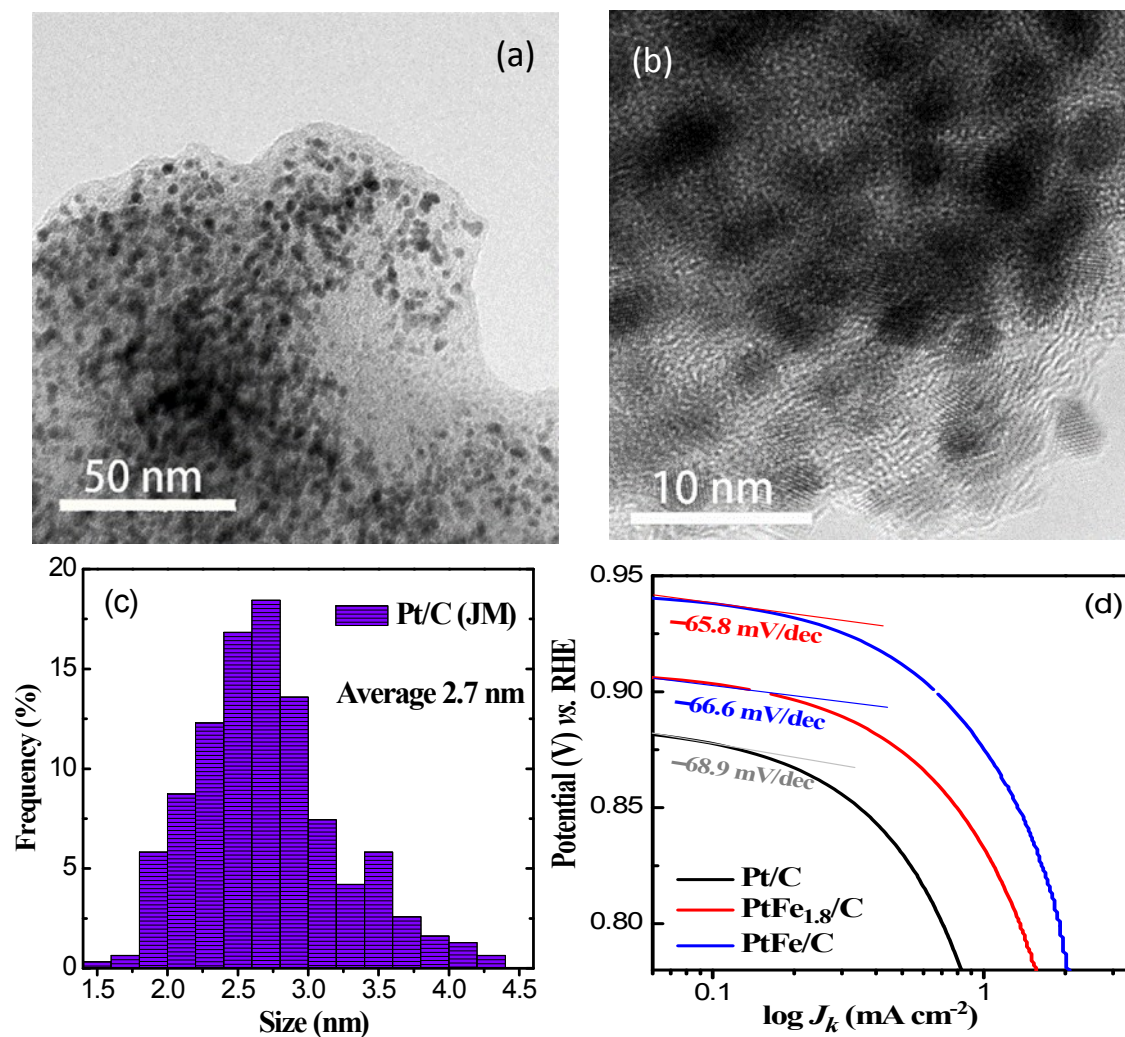
**Fig. S1.** Grain size distributions measured from TEM images for as-deposited (a) and annealed PtFe/C (b).

Fig. S2. N_2 adsorption/desorption isotherms (a), mesopore size distributions (BJH method) (b) of the porous carbon and the PtFe/C catalyst, and TEM images of the porous carbon (c, d).

Fig. S3. XRD patterns for PtFe and PtFe$_{1.8}$ samples in their as-deposited states.

Fig. S4. (a, b) Typical TEM images of JM Pt/C catalyst, (c) Pt particle size distribution, and (d) Tafel plots (the potential versus the logarithm of the kinetic current density) of different catalysts derived from the ORR curves in Fig. 4a.
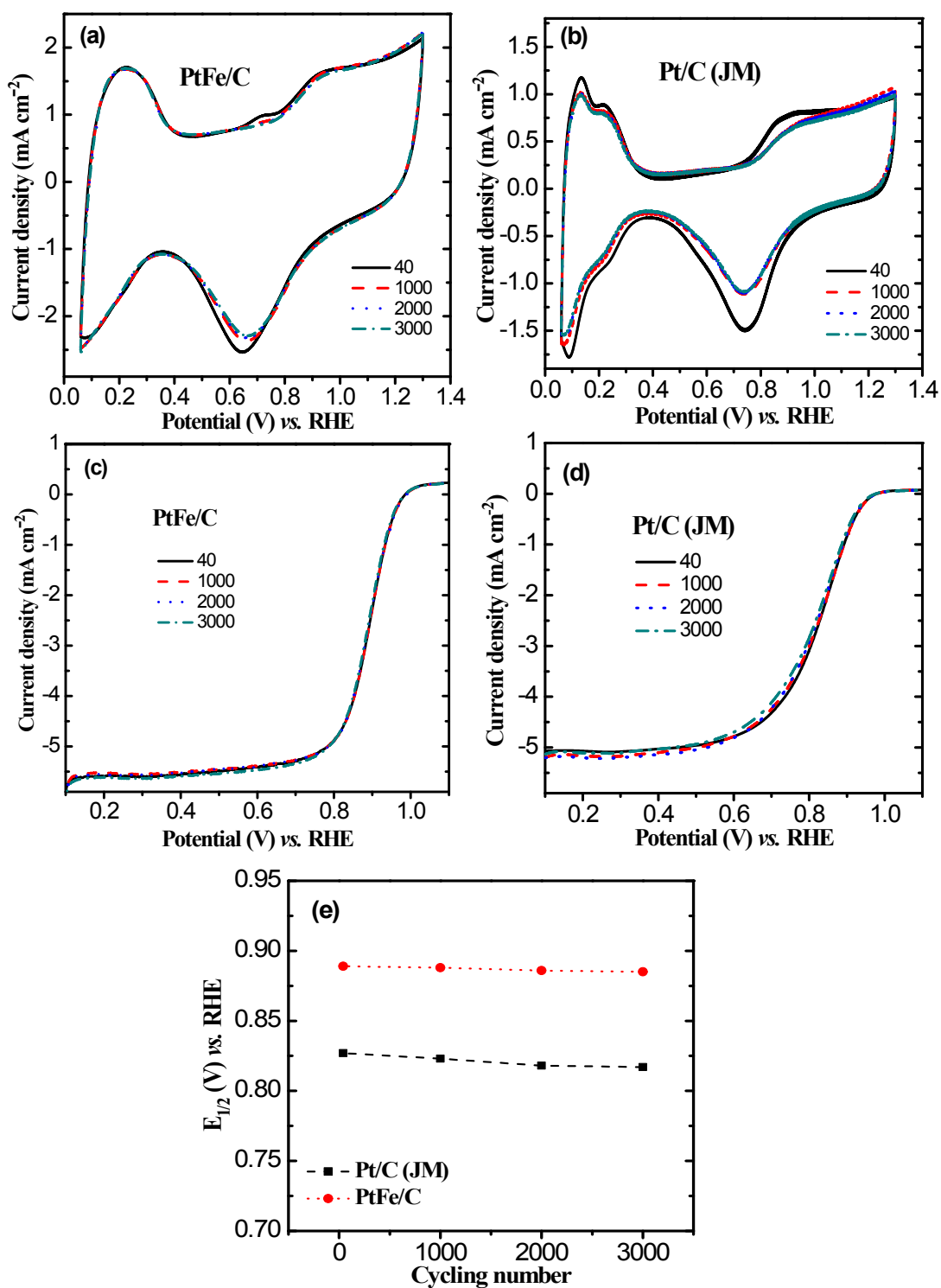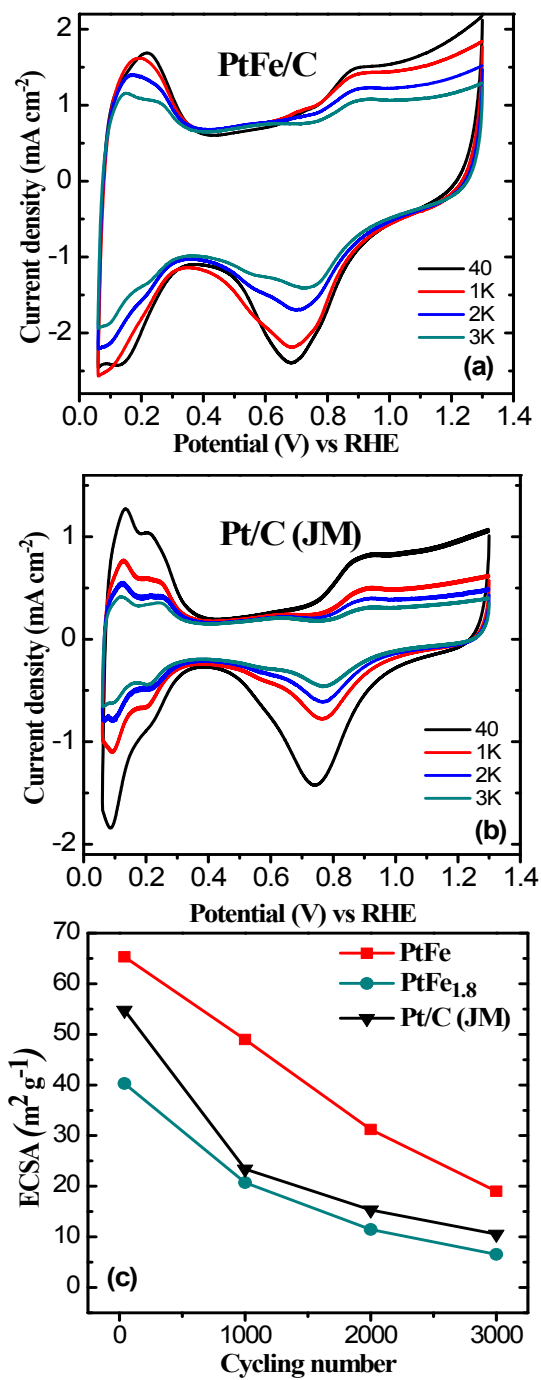
Fig. S5. Potential cycling between 0.6 and 1.0 V. (a, b) CV curves for PtFe/C and Pt/C, respectively. (c, d) ORR polarization curves for PtFe/C and Pt/C, respectively. (e) Variations of half-wave potential with cycling number.
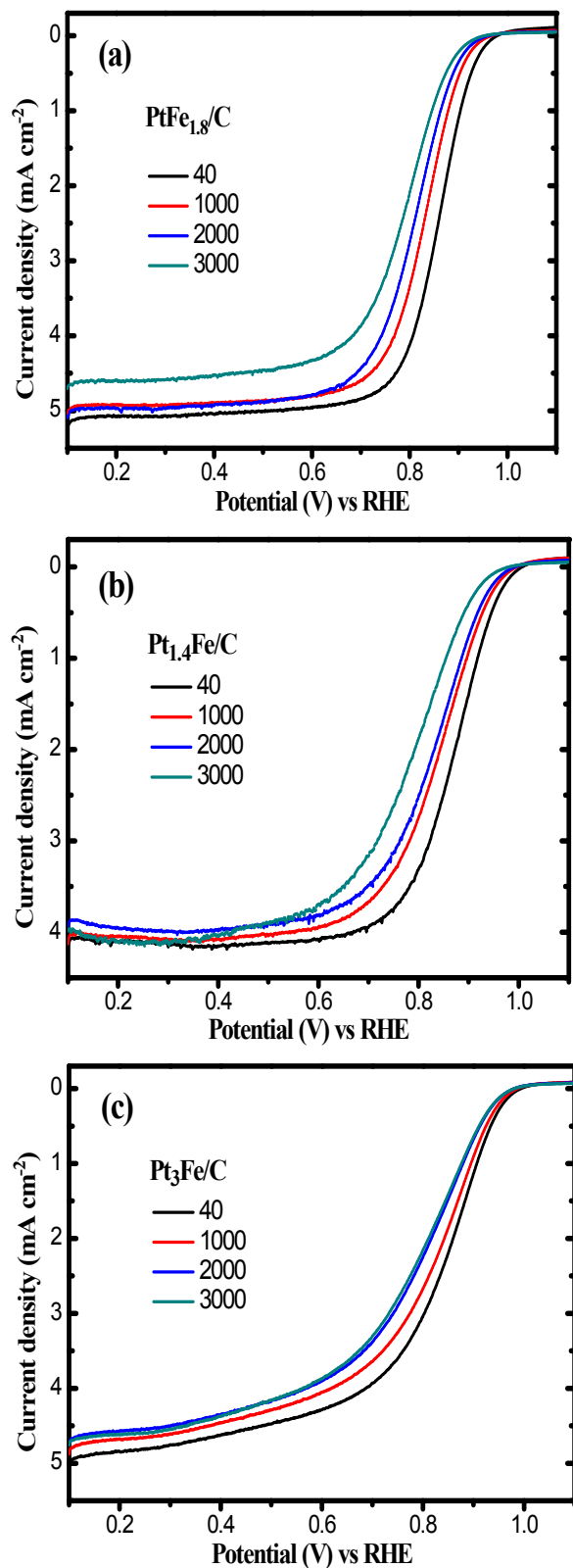
Fig. S6. ORR polarization curves for various numbers of accelerated durability test for PtFe$_{1.8}$/C (a), PtFe$_{1.4}$/C (b), and Pt$_3$Fe/C (c). Potential cycling: 0.66-1.3 V.

Fig. S7. (a, b) CV curves obtained by cycling the potential from 0.66 to 1.3 V for PtFe/C and Pt/C, respectively. (c) Comparison of electrocatalytic surface areas (ECSA) for various numbers of potential cycling among different catalysts.
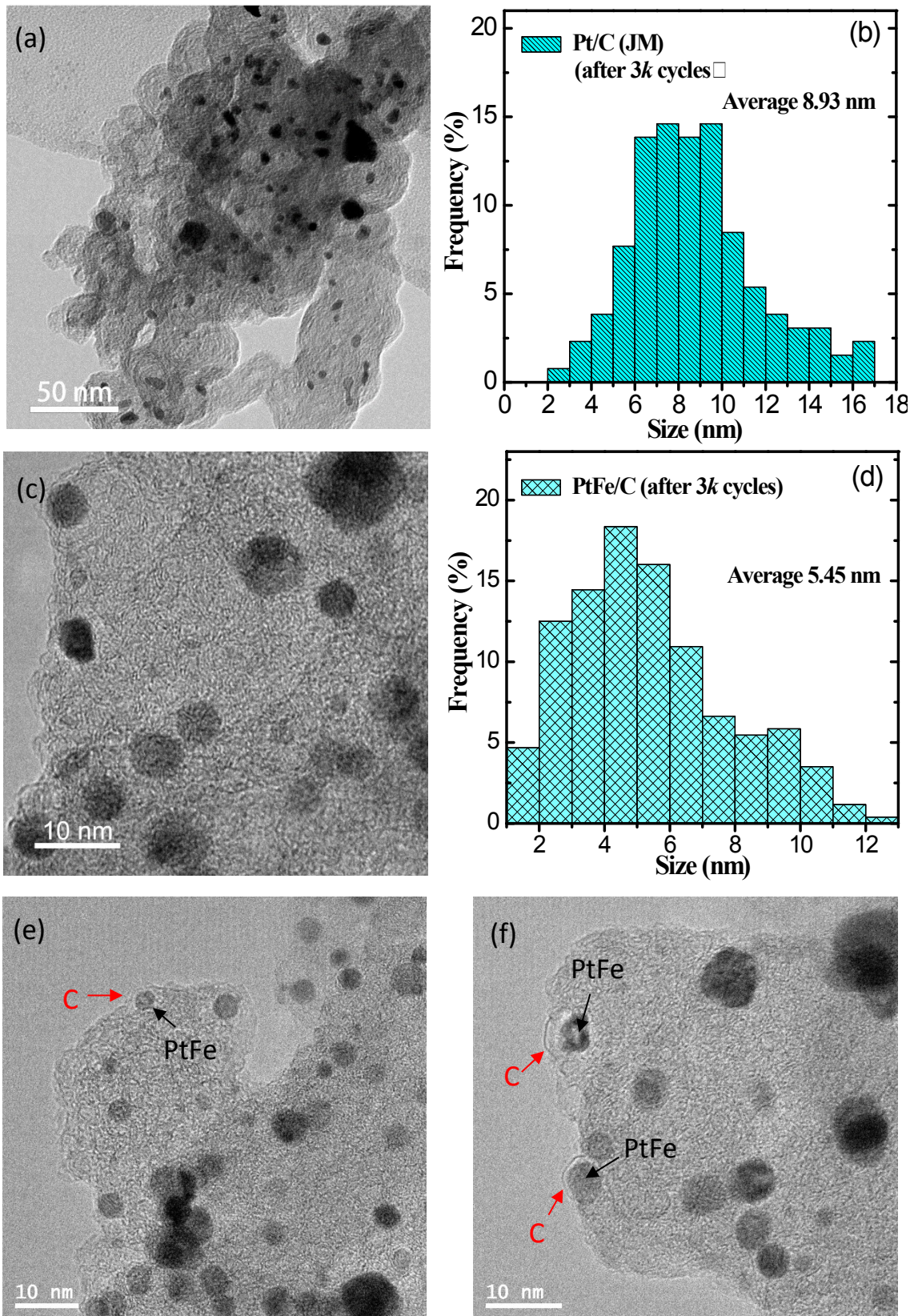
Fig. S8. (a) Typical TEM image and (b) particle size distribution of Pt/C catalyst after 3000 cycles, (c, e, f) TEM images and (d) particle size distribution of PtFe catalyst after 3000 cycles. Note that the PtFe particles were still entrapped in carbon cages after the cycling, as marked by the red arrows.